European Journal of Neuroscience, Vol. 19, pp. 1773–1788, 2004

Modulation of photic resetting in rats by lesions of projections to the suprachiasmatic nuclei expressing p75 neurotrophin receptor

Christine Erhardt,[1] Rodrigue Galani,[2] Hélène Jeltsch,[2] Jean-Christophe Cassel,[2] Paul Klosen,[1] Jérôme S. Menet,[1] Paul Pévet[1] and Etienne Challet[1]

[1]Laboratory of Neurobiology of Rhythms, Centre National de la Recherche Scientifique (UMR7518), Department of Neuroscience (IFR37), University Louis Pasteur, 12 rue de l'université, 67000 Strasbourg, France

[2]Laboratory of Behavioural and Cognitive Neuroscience, CNRS UMR 7521, University Louis Pasteur, Strasbourg, France

Keywords: 192 IgG-saporin, acetylcholine, basal forebrain, circadian rhythm

Abstract

The suprachiasmatic nuclei of the hypothalamus (SCN) are the site of the master circadian clock in mammals. The SCN clock is mainly entrained by the light–dark cycle. Light information is conveyed from the retina to the SCN through direct, retinohypothalamic fibres. The SCN also receive other projections, like cholinergic fibres from basal forebrain. To test whether cholinergic afferents are involved in photic resetting, lesions of cholinergic projections were performed in rats with intracerebroventricular (i.c.v.) injections or intra-SCN microinjections of 192 IgG-saporin. When injected in the SCN, this immunotoxin destroys the cholinergic projections and retinohypothalamic afferents that express p75 low-affinity nerve growth factor ($p75^{NGF}$) receptors. The extent of lesions in the basal forebrain and SCN was assessed by acetylcholinesterase histochemistry, $p75^{NGF}$ receptor, choline acetyl-transferase, calbindin-D28K and VIP immunocytochemistry. The intra-SCN treatment reduced light-induced phase advances by 30%, and induced a complete loss of forebrain and retinal afferents expressing $p75^{NGF}$ receptors within the SCN and a decrease of forebrain cholinergic neurons, most likely those projecting to the SCN. The i.c.v. treatment reduced light-induced phase advances by 40%, increased phase delays and led to extensive damage of forebrain $p75^{NGF}$-expressing neurons, while sparing half of the fibres expressing $p75^{NGF}$ receptors (retinal afferents?) in the SCN. Because the integrity of forebrain $p75^{NGF}$-expressing neurons appears to be critical in mediating the effects on light-induced phase advances, we therefore suggest that anterior cholinergic projections expressing $p75^{NGF}$ receptors modulate the sensitivity of the SCN clock to the phase advancing effects of light.

Introduction

In mammals, most of the behavioural and physiological processes express a rhythmicity of approximately 24 h, generated by a circadian clock in the suprachiasmatic nuclei (SCN). This biological clock can be synchronized by several photic and nonphotic cues. Among them, light is the most potent synchronizing factor. Entrainment of the SCN clock to the light–dark cycle is mediated by at least two neural pathways: the retino-hypothalamic tract, and the geniculo-hypothalamic tract via the intergeniculate leaflet (Morin, 1994). The SCN may also receive indirect photic information from other structures, such as the midbrain raphe (Shen & Semba, 1994; Kawano *et al*., 1996) and basal forebrain nuclei (Youngstrom *et al*., 1991; Bina *et al*., 1993), which send serotonergic and cholinergic fibres to the SCN, respectively (Bina *et al*., 1993; Morin, 1994).

Cholinergic terminals have been localized in the SCN by visualization of synaptic connections (Kiss & Halasz, 1996) and choline acetyltransferase (ChAT; van den Pol & Tsujimoto, 1985). Muscarinic and nicotinic receptors have been identified in the SCN region (van der Zee *et al*., 1991). The cholinergic projections to the SCN originate from the basal forebrain, especially the nucleus basalis magnocellularis, the diagonal band of Broca and the medial septum, and the brainstem, including the pedunculopontine tegmental nucleus and the parabigeminal nucleus (Bina *et al*., 1993).

These cholinergic projections may affect the regulation of photic synchronization. A nocturnal light exposure produces a marked release of acetylcholine in the rat SCN (Murakami *et al*., 1984). Moreover, *in vivo* injections of carbachol, a nonspecific cholinergic agonist, mimic light masking (Zatz & Brownstein, 1979; Miller & Billiar, 1986; Takeuchi *et al*., 1993) and photic phase shifting (Zatz & Herkenham, 1981; Mistlberger & Rusak, 1986; Wee *et al*., 1992; Colwell *et al*., 1993; Abbott *et al*., 2002), although nonphotic-like phase shifting (i.e. occurring during daytime) was also reported (Meijer *et al*., 1988).

Cholinergic drugs more selective than carbachol were also used in the present context. Injections of nicotine led to induction of c-FOS in the SCN (Ferguson *et al*., 1999) and photic-like phase shifting effects that can be blocked with mecamylamine, a cholinergic antagonist (Keefe *et al*., 1987; O'Hara *et al*., 1998). Mecamylamine also blocks light-induced c-FOS expression in the SCN (Zhang *et al*., 1993). *In vitro* administration of nicotine at most circadian times or carbachol in late night induces phase advances in the neuronal activity of rat SCN slices (Trachsel *et al*., 1995). Moreover, application of acetylcholine

Correspondence: Dr E. Challet, as above.
E-mail: challet@neurochem.u-strasb.fr

Received 18 July 2003, revised 17 December 2003, accepted 15 January 2004

doi:10.1111/j.1460-9568.2004.03281.x

and muscarinic agonists during the night leads to phase advances in the SCN neuronal activity (Liu & Gillette, 1996).

These studies using cholinergic agonists therefore suggest that acetylcholine release modulates photic resetting. We attempted to provide novel experimental data to support this hypothesis by lesioning basal forebrain cholinergic projections to the SCN in the rat. This was achieved with intracerebroventricular (i.c.v.) or intra-SCN injections of 192 IgG-saporin, a cholinergic immunotoxin (Leanza *et al*., 1995), and assessment of circadian rhythms of locomotor activity and core temperature and their responses to light.

Materials and methods

Animals and laboratory conditions

Eight-week-old male Long-Evans rats (Janvier, Le Genest St Isle, France) were maintained in a temperature-controlled room ($23 \pm 1\,^{\circ}C$) and initially exposed to a daily 12-h light/12-h dark cycle (lights on at 07:00 h). During the daytime, light intensity was 100 lux at the level of the cages. During the night, there was a dim red light ≤ 1 lux at the level of the cages. Food and water were available *ad libitum* throughout the experiment. All experiments were performed in accordance with 'Principles of laboratory animal care' (NIH pub. No. 86-23, revised 1985) as well as the French national laws.

Surgery

All lesions were performed with 192 IgG-saporin, a cholinergic immunotoxin. 192 IgG-saporin is a ribosome inactivating protein (saporin) coupled to a monoclonal antibody (192-IgG), specific for the rat p75 low-affinity nerve growth factor ($p75^{NGF}$) receptor. Following i.c.v. administration, this neurotoxin is internalized by terminals and accumulates in cell bodies after retrograde transport (Leanza *et al*., 1995). Based on the observation that basal forebrain cholinergic neurons express $p75^{NGF}$ receptor, this immunotoxin has been widely used selectively to lesion cholinergic neurons of the basal nuclear complex. Following i.c.v. administration in rats, 192 IgG-saporin allows extensive (more than 95%), dose-dependent and selective destruction of cholinergic neurons in the basal forebrain without lesioning other neurotransmitter systems, nor cholinergic neurons of the brainstem, cerebellum and spinal cord that do not express $p75^{NGF}$ receptor (Leanza *et al*., 1995).

i.c.v. 192 IgG-saporin injection

In the first experiment, 24 rats were randomly divided into two groups. The animals were 4 months old at the time of the surgery. Surgery was conducted under deep anaesthesia with i.p. injection of ketamine (50 mg/kg; Imalgène, Mérieux, Lyon, France) and xylazine (10 mg/kg; Rompun, Bayer Pharma, Puteaux, France). 192 IgG-saporin (lot no. 21-107, Advanced Targeting Systems, San Diego, CA, USA) was diluted in phosphate-buffered saline (PBS) at 1 μg/μL and a dose of 3 μg was injected in each lateral ventricle with a 10-μL Hamilton syringe at the following coordinates: anteroposterior: −0.8 mm from bregma, lateral: ±1.4 mm from the midline, and dorsoventral: −4.3 mm from the skull surface, with the incisor bar set at the interauricular level. The syringe was left in place for 5 min and withdrawn step by step to allow toxin diffusion and prevent backflow. Control rats underwent the same procedure, except that 3 μL of PBS was injected in each lateral ventricle. Because three animals died following anaesthesia, only nine rats were used as controls.

Intra-SCN 192 IgG-saporin injections

In the second experiment, 16 rats were randomized into two groups. The animals were 4 months old at the time of the surgery. Because we faced an unexpected rate of mortality with the ketamine/xylazine anaesthesia in the first series, surgery of the second group was performed under anaesthesia with i.p. injection of equithesine (4.0 mL/kg) as we have previously used in the same rat strain (e.g. Pitrosky *et al*., 1999; Lehmann *et al*., 2000). The incisor bar was set at +5 mm. One microgramme of 192 IgG-saporin (lot no. 21-107) diluted in 1 μL of PBS was injected in each SCN through a glass micropipette (tip diameter 30 μm) connected to a 1-μL Hamilton syringe at the following coordinates: anteroposterior: 1.8 mm from bregma, lateral: ±0.5 mm from the midline, dorsoventral: −8.3 mm (at 2°) ventral to dura. The pipette was then left in place for 5 min and withdrawn with gradual steps. The surgical procedure was similar for control rats, except that 1 μL of PBS was injected in each SCN. Nine and seven rats were injected with 192 IgG-saporin and PBS, respectively.

Circadian rhythms

Telemetry

Eight and 15 days before i.c.v. and intra-SCN injections, respectively, the animals were transferred to individual cages equipped with a running wheel (diameter 30 cm) that closed a microswitch on each revolution. Eight days before i.c.v. or intra-SCN injections, rats were i.p. implanted under gaseous anaesthesia (mixture of O_2, nitrogen protoxide and isoflurane) with MiniMitter telemetry devices (MiniMitter Co., Sunriver, USA) to record body temperature. Body temperature and wheel-running activity were recorded every 5 min (Dataquest III acquisition system; Data Sciences Co., St Paul, MN, USA). Zeitgeber time (ZT) 12 is defined as the onset of the dark period for animals under a light–dark cycle. Circadian time (CT) 12 is defined as the onset of the locomotor activity rhythm for nocturnal animals under constant darkness.

Experimental protocol

After i.c.v. and intra-SCN injections, the animals underwent the same experimental conditions. Rats were first housed under a light–dark cycle up to 6 weeks after surgery to determine the temporal organization of circadian rhythms and the general response to photic entrainment. The animals were then housed in constant darkness for 8 weeks in order to study the effects of the lesions on the endogenous period of the circadian rhythms. To assess the effects of the lesions on light-induced phase shifts, after 2 weeks in constant darkness, the animals were exposed to a light pulse started at CT21. Two weeks later, they were exposed to a light pulse started at CT14. For light stimulation, rats were transferred individually from their own cages to a white chamber inside a photic stimulation device that delivers a 100-lux light pulse over a period of 30 min. After 8 weeks in constant darkness, the animals were exposed back to a light–dark cycle for 10 days.

Methods of analysis

Onsets and offsets of the daily pattern of locomotor activity and body temperature were determined with ClockLab (Actimetrics, Evanston, USA) over 8 days before and 3 weeks after lesion. During these periods, the average numbers of wheel revolutions were determined per day, during the light period (i.e. from 07:00 to 19:00 h) and during the dark period (i.e. from 19:00 to 07:00 h) by using the activity profile window (ClockLab). The free-running period (τ) was determined using a χ^2 periodogram (ClockLab) over three periods of 10 days in constant darkness (i.e. before the first light pulse, before and after the second light pulse). The magnitude and direction of light-induced phase shifts were estimated by two linear regressions considering the 10 days before and after the light pulse (ClockLab). The phase shifts were determined as the difference between the lines fitted to activity and temperature onsets before and after light exposure.

Tissue preparation, histochemistry and immunocytochemistry

Tissue preparation

The animals were killed 4 months after surgery. The rats were deeply anaesthetized with i.p. injection of pentobarbital, and perfused transcardially with 200 mL of 0.9% saline (4 °C) followed by 300 mL of 4% paraformaldehyde in PBS maintained at 4 °C. Brains were immediately removed and postfixed overnight before transfer to a 30% sucrose solution for 72 h at 4 °C. Brains were then frozen in isopentane at −60 °C and stored at −80 °C. Four series of 30-μm coronal cryosections through the nucleus basalis magnocellularis, the diagonal band of Broca and the SCN were prepared on a cryostat at −19 °C and collected in PBS. The localization of these structures was determined according to the rat brain atlas of Paxinos & Watson (1986). One series of free-floating sections was stained with cresyl violet. The three other series were processed for acetylcholinesterase (AChE) histochemistry, $p75^{NGF}$ receptor immunocytochemistry and vasoactive intestinal peptide (VIP) immunocytochemistry.

AChE histochemistry

Based on the observation that AChE is predominantly localized in cholinergic neurons within the central nervous system (Butcher & Woolf, 1984), we used AChE histochemistry according to the protocol for fibres established by Di Patre *et al*. (1993) to confirm lesions of cholinegic fibres and terminals after 192 IgG-saporin administration. Brain sections were washed in PBS and permeabilized in 0.1% Triton X100 diluted in cold PBS. Further incubations were processed at room temperature, with gentle agitation. The sections were washed again in 1 M PBS and 50 mM Tris-Maleate (pH 5.7) and were then incubated in a Karnovsky-Roots medium (32.5 mM Tris-maleate, 5 mM sodium citrate, 3 mM cupric sulphate, 0.5 mM potassium ferricyanide, 1.83 mM acetylcholine iodide; Sigma, St Louis, MO, USA). After incubation in Karnovsky-Roots medium for 15 min, sections were washed and stained by incubation in a solution containing 3,3′-diaminobenzidine-nickel ammonium sulphite and 3% hydrogen peroxide (2 μL/mL) solution. The specificity of the staining was assessed on control sections with iso-OMPA (30 μM, butyrylcholinesterase inhibitor, Sigma) and BW284c51 (10 μM, AChE inhibitor, Sigma). After completion of the staining, sections were washed in PBS and mounted on glass slides coated with gelatin. Mounted sections were dehydrated in a graded ethanol series, cleared in xylene for 5 min and coverslipped.

$P75^{NGF}$ receptor, ChAT, calbindin-D28K and VIP immunocytochemistry

Sections through the entire rostro-caudal extent of the SCN and a few sections of the forebrain, including the nucleus basalis magnocellularis (NBM), the vertical limb (vDBB) and the horizontal limb (hDBB) of the diagonal band of Broca were processed for $p75^{NGF}$ receptor (experiments 1 and 2) and for ChAT (experiment 2) immunocytochemistry. Sections through the SCN were also processed for VIP (vasoactive intestinal peptide; experiments 1 and 2) and calbindin-D28K (CalB; experiment 2) immunocytochemistry. Free-floating sections were washed in Tris-NaCl buffer (TBS) and permeabilized in a phosphate-buffered ethanol series (10, 15 and 20%). Sections were then incubated in TBS, 0.3% hydrogen peroxide and 0.1% NaN_3 to inactivate endogenous peroxidase activity. After preincubation for 1 h in TBS + 10% fetal bovine serum and 0.05% Tween 20 (Tw20), the sections were incubated with the primary antibody (mouse anti-$p75^{NGF}$ receptor monoclonal antibody, Chemicon International, diluted 1 : 1000; rabbit anti-VIP, Niepke, Netherlands Institute for Brain Research, Amsterdam, diluted 1 : 2000; goat anti-ChAT, Chemicon International, diluted 1 : 10 000; or mouse anti-CalB, Sigma; diluted 1 : 10 000) diluted in TBS–Tw20–1% fetal bovine serum overnight with gentle agitation at room temperature. Thereafter, sections were rinsed in TBS–Tw20 and incubated with biotinylated sheep anti-mouse IgG (Amersham, diluted 1 : 2000 for $p75^{NGF}$ receptor), biotinylated donkey anti-rabbit IgG (Jackson, diluted 1 : 2000 for VIP), biotinylated donkey anti-goat IgG (Amersham, diluted 1 : 1000 for ChAT), or biotinylated rabbit anti-mouse IgG (Dako, diluted 1 : 1000 for CalB) for 1 h. After several washes in TBS–Tw20, the sections were incubated with streptavidin-peroxidase (Roche, diluted 1 : 2000) in a solution of TBS–Tw20 + 0.2% cold water fish skin gelatin (Sigma) for 1 h. The sections were rinsed with TBS–Tw20 followed by TBI (50 mM Tris, 10 mM Imidazole, pH 7.6). Sections of SCN for ChAT and calb were pretreated with acetate cobalt to intensify the colour of the diaminobenzidine reaction product. The sections were then transferred to a solution of 3,3′-diaminobenzidine (Sigma, 0.5 mg/mL, diluted in TBI) to which 0.003% hydrogen peroxide was added after 5 min. After completion of the peroxidase detection, the sections were rinsed in TBS, mounted on gelatin-coated slides, dehydrated and coverslipped.

Quantification of staining signals

To assess the extent of the lesions of basal forebrain cholinergic neurons, $p75^{NGF}$ receptor (for experiments 1 and 2) and ChAT (for experiment 2) immunoreactive cells were counted on one section of the vDBB, of the hDBB and of the NBM per animal. These forebrain regions were chosen because they have been demonstrated to contain neurons that express $p75^{NGF}$ receptors and project to the SCN (Bina *et al*., 1997). Immunoreactive cells to CalB were also counted in the SCN. Measures of the optical density (OD) of the staining were also realized for each brain in order to quantify staining intensity after AChE histochemistry in the frontoparietal cortex, as well as density of VIP and $p75^{NGF}$ receptor immunoreactive fibres/terminals in the SCN. Densitometric analysis was performed with an image analysis system (Biocom, Rag 200, Les Ulis, France). The specific staining was calculated by subtracting the intensity staining of background from that of the area of interest. For AChE staining in the cortex, OD was measured by subtraction of the background measured in the corpus callosum from OD measured in the cerebral cortex. For $p75^{NGF}$ receptor and VIP staining in the SCN, OD was measured by subtraction of the background measured in the anterior hypothalamic area above the SCN from the averaged OD measured in the left and the right SCN. Data are expressed as relative OD values.

Statistical analysis

Values are presented as means ± SEM. Data were analysed by two-way analyses of variance (ANOVA) with repeated measures to compare the effects of the immunotoxin (192 IgG-saporin vs. PBS) and the different periods (before vs. after lesion). When only two groups were compared (192 IgG-saporin vs. PBS), Student's *t*-test was used to compare the means. Because the two experiments (i.c.v. and intra-SCN injections of 192 IgG-saporin) were performed independently, no attempt was made to compare interexperiment groups.

Results

AChE histochemistry

i.c.v. injections of 192 IgG-saporin

In control animals, the staining observed in the cerebral cortex was very similar with or without incubation with iso-OMPA, an inhibitor of butyrylcholinesterase (data not shown). This lack of difference confirms the specificity of the method used. In the cerebral cortex of

control rats, incubation with BW284c51, an inhibitor of AChE, resulted in the disappearance of AChE staining (data not shown). The protocol allowed clear visualization of dendrites and neurites, as well as cell bodies in the basal nuclear complex, the cerebral cortex (Fig. 1A–D) and the striatum. In sections from control rats, we observed a dense network of fibres and a few cell bodies in the cerebral cortex (Fig. 1A and C). 192 IgG-saporin injected i.c.v. induced a marked decrease of OD in the cortex of the lesioned rats compared with control animals (6.4 ± 0.8 vs. 21.6 ± 1.6 arbitrary units (a.u.), $n = 12$ and 9, respectively; $t_{19} = 9.2$, $P < 0.01$; Fig. 1B and D), in spite of the persistence of isolated cell bodies, probably corresponding to noncholinergic interneurons (Levey *et al.*, 1984). In the SCN, however, the contrast between stained fibres and background was too slight to detect any sizeable OD difference between control and i.c.v. lesioned rats (Fig. 1E and F).

Intra-SCN injections of 192 IgG-saporin

The staining in cerebral cortex was similar between control and lesioned animals (18.2 ± 2 vs. 17.2 ± 1.9 a.u., $n = 7$ in both groups; $t_{12} = 0.5$; $P > 0.1$). Incubations of sections with either iso-OMPA or

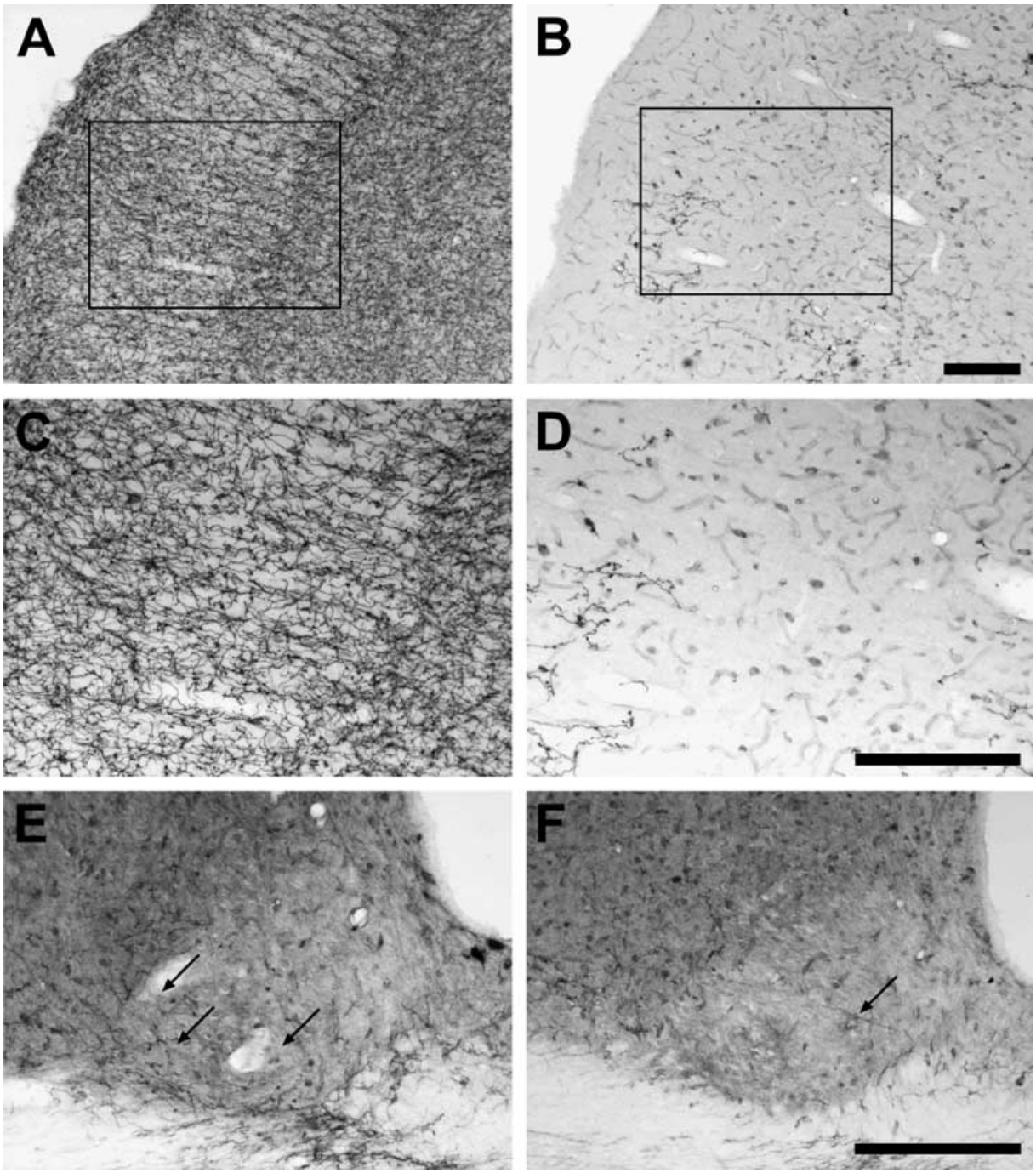

FIG. 1. Acetylcholinesterase-positive staining in the frontoparietal cortex (A–D) and the suprachiasmatic nuclei (E and F) in rats given vehicle (left panels) or i.c.v. 192 IgG-saporin (right panels) injections. C and D are enlarged views of A and B, respectively. Arrows in E and F indicate acetylcholinesterase-positive fibres. Scale bars, 200 μm.

BW284c51 gave results similar to those mentioned earlier (data not shown). Again, in the SCN, the contrast between stained fibres and background was too weak to detect a difference between control and lesioned animals (data not shown).

P75^{NGF} receptor (experiments 1 and 2) and ChAT (experiment 2) immunocytochemistry

i.c.v. injections of 192 IgG-saporin

In control rats, we observed p75^{NGF} receptor immunoreactive cell bodies in vDBB, hDBB and NBM (Fig. 2A, C and E, respectively). The number of immunoreactive cells in hDBB, vDBB and NBM (Fig. 2B, D and F, respectively) was reduced by 90% or more in rats with i.c.v. injections of 192 IgG-saporin compared with that in control animals (see Table 1 for values). Staining with cresyl violet, however, showed no widespread nonspecific neuronal loss in the forebrain of animals injected i.c.v. with 192 IgG-saporin (Fig. 3B, D and F) compared with control animals injected with vehicle (Fig. 3A, C and E). In control rats, a strong p75^{NGF} receptor immunostaining was observed on fibres and terminals in the SCN, restricted to their ventrolateral region (Fig. 4A). Immunostaining in the SCN was only decreased by 50% in lesioned animals compared with that in control rats (8.1 ± 2.7 vs.

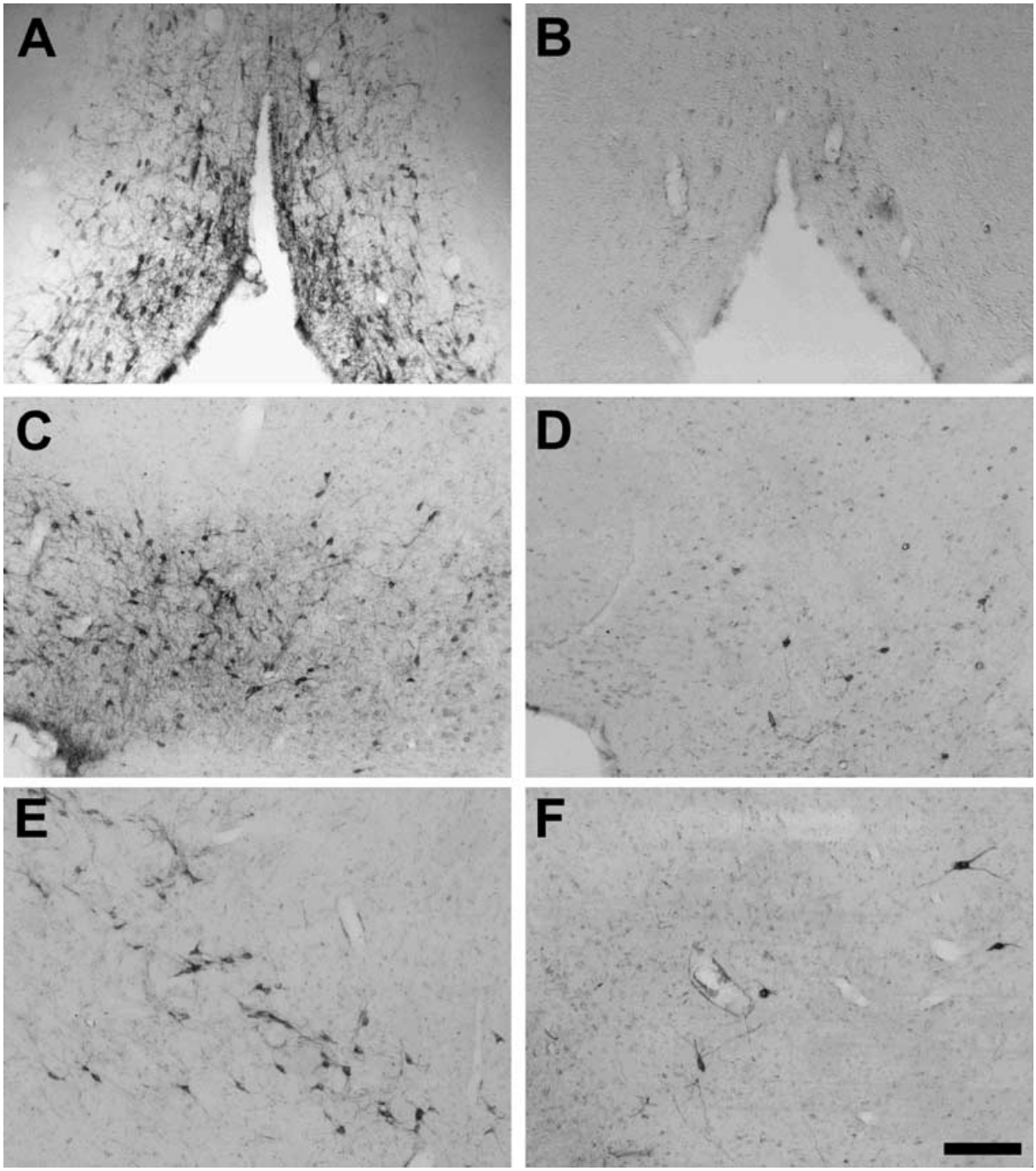

FIG. 2. p75 low-affinity nerve growth factor receptor immunostaining in the vertical (A and B) and horizontal (C and D) limbs of the diagonal band of Broca and the nucleus basalis magnocellularis (E and F) in rats given vehicle (left panels) or i.c.v. 192 IgG-saporin (right panels) injections. Scale bar, 200 μm.

TABLE 1. The number of immunoreactive cells to $p75^{NGF}$ receptor in the basal forebrain

	Control i.c.v. ($n=9$)	Saporin i.c.v. ($n=12$)	Control intra-SCN ($n=7$)	Saporin intra-SCN ($n=7$)
vDBB	103 ± 11	$11 \pm 3^{*}$	89 ± 12	$52 \pm 7^{*}$
hDBB	70 ± 6	$5 \pm 1^{*}$	74 ± 2	$62 \pm 2^{*}$
NBM	50 ± 1	$5 \pm 1^{*}$	48 ± 1	$39 \pm 2^{*}$

$^{*}P < 0.05$ between 192 IgG-saporin treatment and respective control for a given brain region (*t*-test).

16.5 ± 3.6 a.u., $n = 12$ and 9, respectively; $t_{19} = 6.4$, $P < 0.001$; Fig. 4B).

Intra-SCN injections of 192 IgG-saporin

The number of $p75^{NGF}$ receptor immunoreactive cells in vDBB, hDBB and NBM was reduced, respectively, by 44, 26 and 18% in animals with intra-SCN injections of 192 IgG-saporin compared with control rats (Fig. 5A–F; see Table 1 for values). The observed reduction may probably be attributed to a loss of cholinergic neurons, as assessed by the decrease in the number of cell bodies immunoreactive to ChAT by 42, 16 and 19% in vDBB, hDBB (in that case, the reduction did not

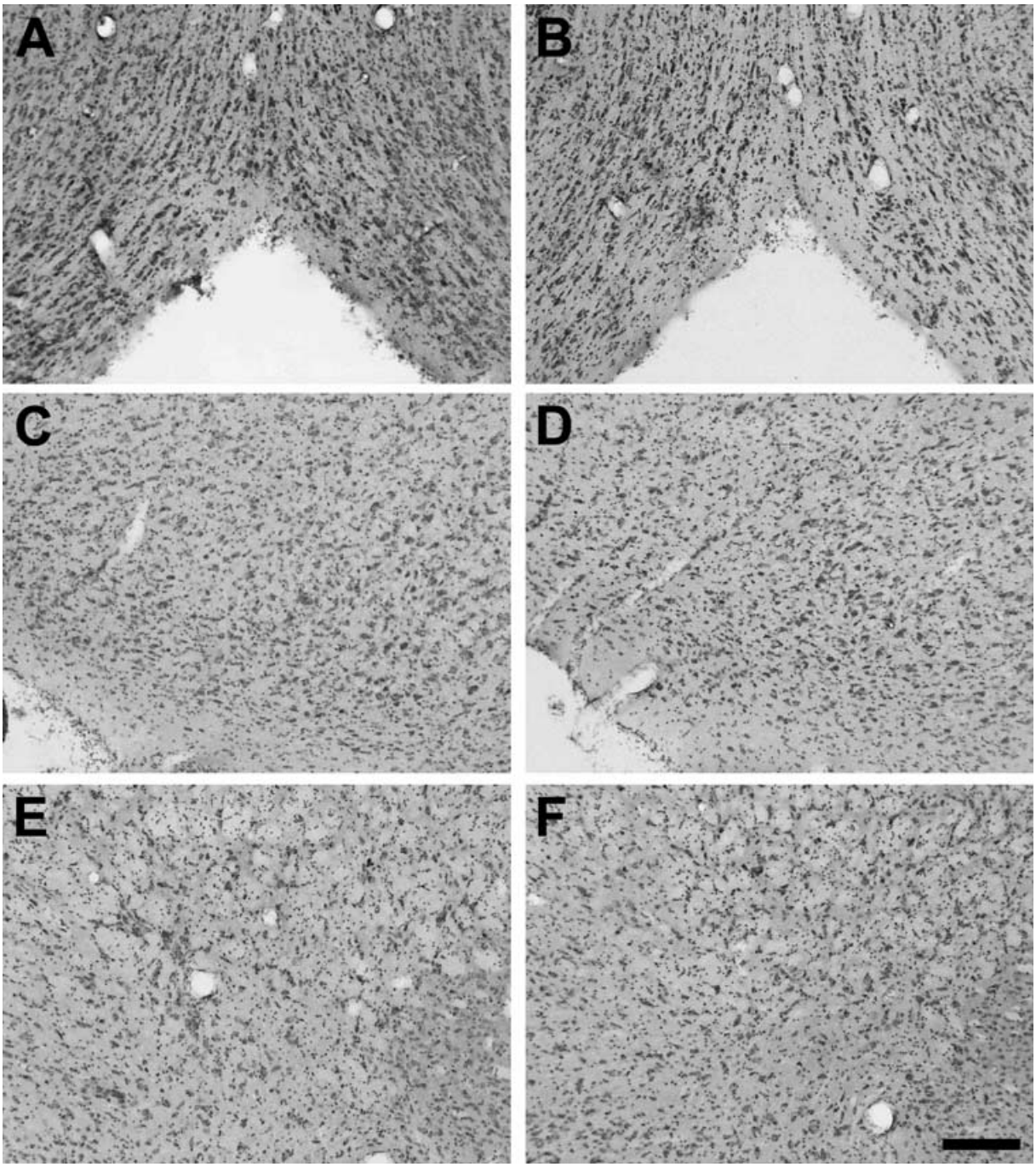

FIG. 3. Cresyl violet staining in the vertical (A and B) and horizontal (C and D) limbs of the diagonal band of Broca and the nucleus basalis magnocellularis (E and F) in rats given vehicle (left panels) or i.c.v. 192 IgG-saporin (right panels) injections. Scale bar, 200 μm.

reach a significant level) and NBM, respectively (Fig. 6A–F; see Table 2 for values). In the control rats, we observed a dense $p75^{NGF}$ receptor immunoreactive staining on fibres and terminals localized in the ventrolateral portion of the SCN (Fig. 7A). In the nine lesioned rats, there was no plexus of $p75^{NGF}$ receptor immunoreactive fibres and terminals, which strongly suggests the destruction of forebrain cholinergic fibres as well as retinal afferents expressing $p75^{NGF}$ receptor and projecting to the SCN (Fig. 7B). We observed, however, a vascular staining in the SCN of four lesioned rats (Fig. 7C). This may be related to an overexpression of $p75^{NGF}$ receptor in response to reactive vascularization induced by local lesions after intra-SCN injections. Indeed, the vascular response to injury is associated with neoangiogenesis and overexpression of neurotrophins and their receptors in the vessels (Cantarella *et al*., 2002). The vascular staining in the SCN prevented us from obtaining a reliable assessment of $p75^{NGF}$ receptor immunostaining on neuronal fibres and terminals in the SCN region. Furthermore, two lesioned rats exhibited hypothalamic damage that included the whole SCN and spread to the optic chiasm (Fig. 7D). These extended lesions were concomitant with behavioural arrhythmicity and the two rats were excluded from the data analysis. Staining

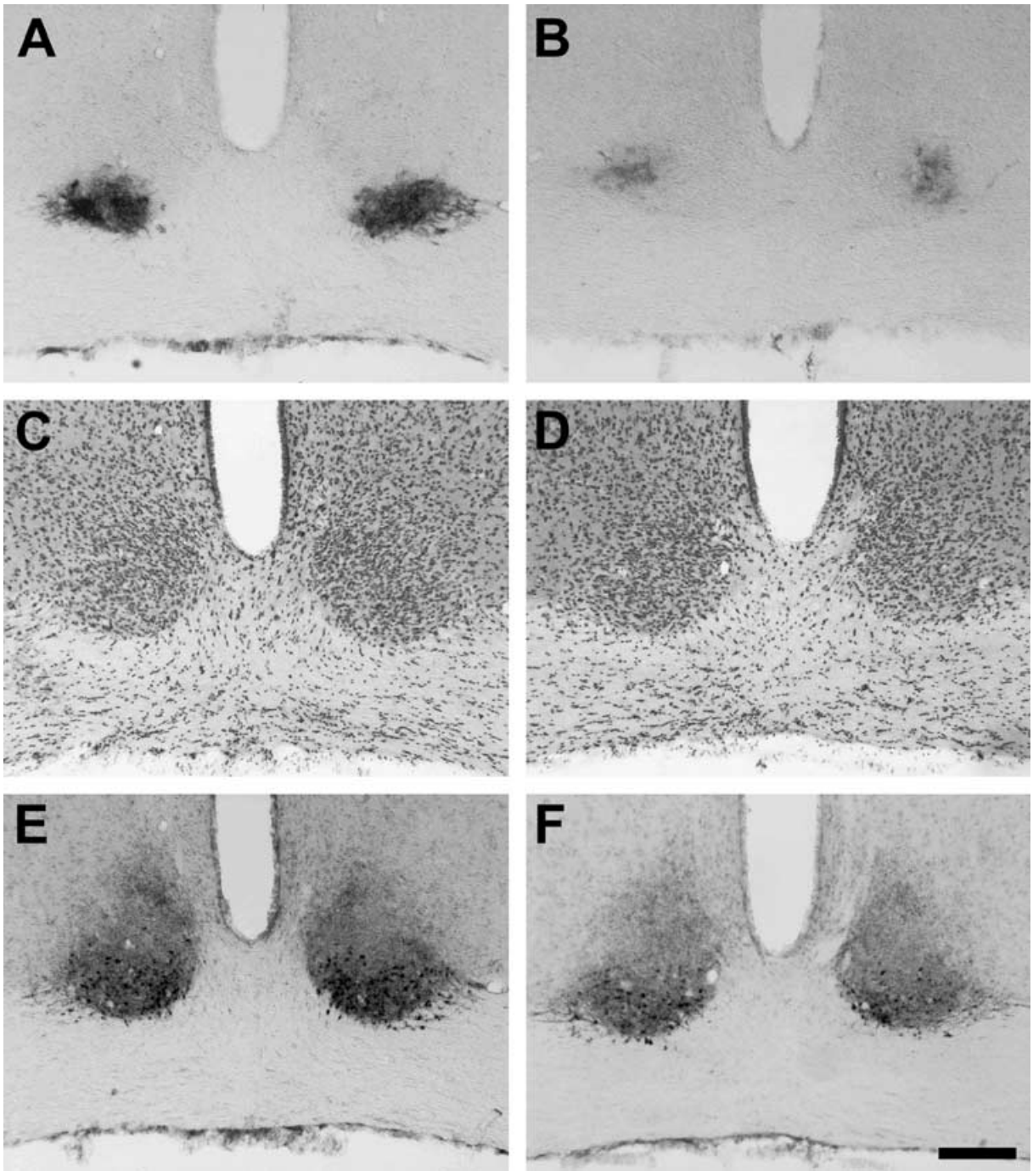

FIG. 4. p75 low-affinity nerve growth factor receptor immunostaining (A and B), cresyl violet staining (C and D) and VIP immunostaining (E and F) in the suprachiasmatic nuclei of rats given vehicle (left panels) or i.c.v. 192 IgG-saporin (right panels) injections. Scale bar, 200 μm.

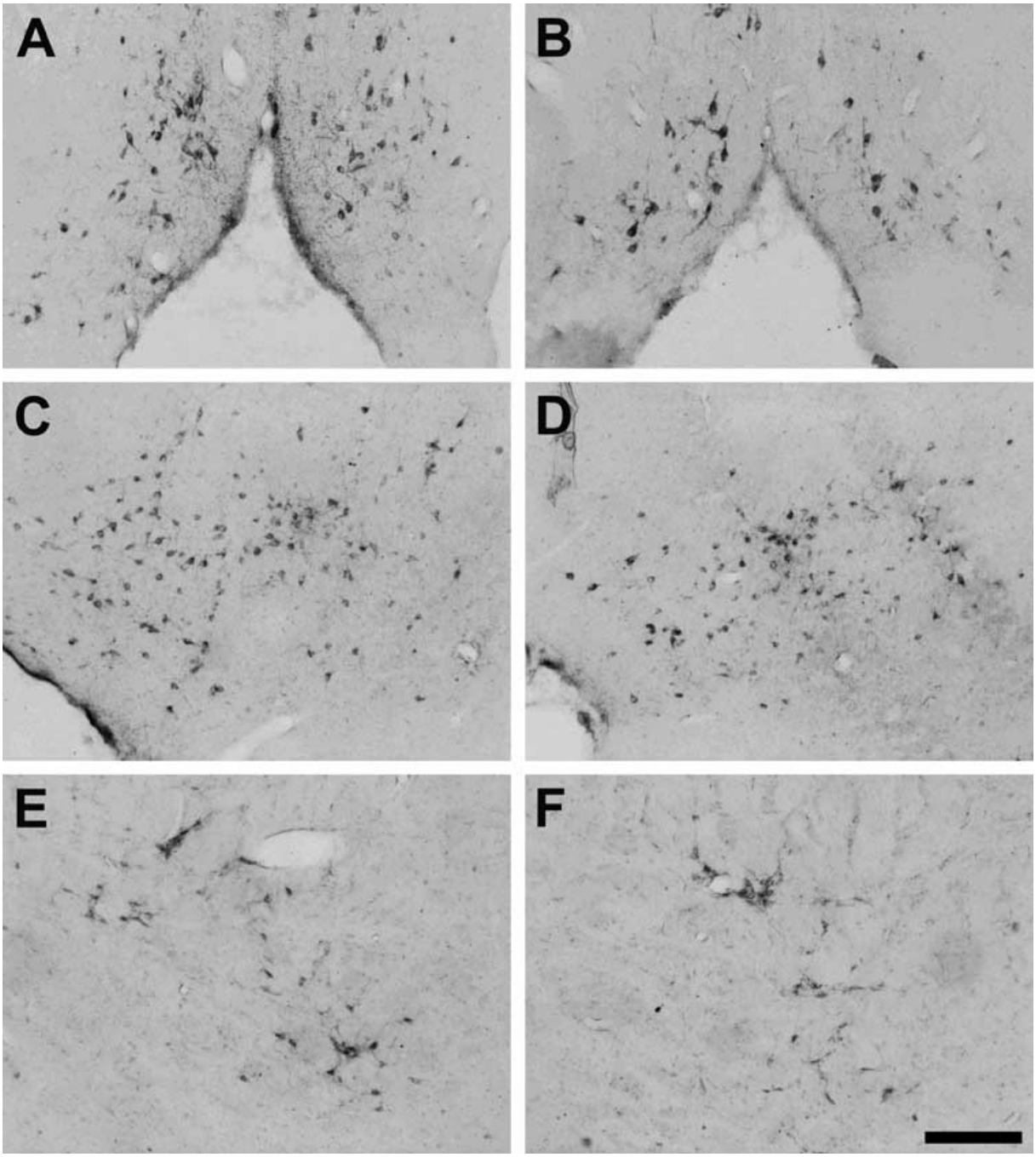

FIG. 5. p75 low-affinity nerve growth factor receptor immunostaining in the vertical (A and B) and horizontal (C and D) limbs of the diagonal band of Broca and the nucleus basalis magnocellularis (E and F) in rats given vehicle treatment (left panels) or intra-SCN injections of 192 IgG-saporin (right panels). Scale bar, 200 μm.

with cresyl violet showed no widespread nonspecific neuronal loss in the forebrain of animals injected in the SCN with 192 IgG-saporin (data not illustrated).

VIP (experiments 1 and 2) and CalB (experiment 2) immunostaining

i.c.v. injections of 192 IgG-saporin

VIP staining was observed on fibres and cell bodies localized in the ventrolateral portion of the SCN of control rats (Fig. 4E). There was no difference in OD between control and lesioned rats (16.5 ± 2.7 vs. 15.4 ± 3.4 a.u., $n = 9$ and 12, respectively; $t_{19} = 1.9$, $P > 0.1$), which confirms the integrity of the SCN cells expressing VIP in rats treated with i.c.v. 192 IgG-saporin (Fig. 4F). $p75^{NGF}$ receptor staining in the SCN overlapped VIP staining, albeit with a greater area in the rostrocaudal extent of the SCN.

Intra-SCN injections of 192 IgG-saporin

VIP staining was observed on both fibres and cell bodies in the ventrolateral SCN with no OD difference between control and lesioned rats (11.2 ± 0.6 vs. 12.5 ± 0.7 a.u., $n = 7$ in both groups; $t_{12} = 1.1$, $P > 0.1$; data not illustrated). In addition, the number of CalB-positive

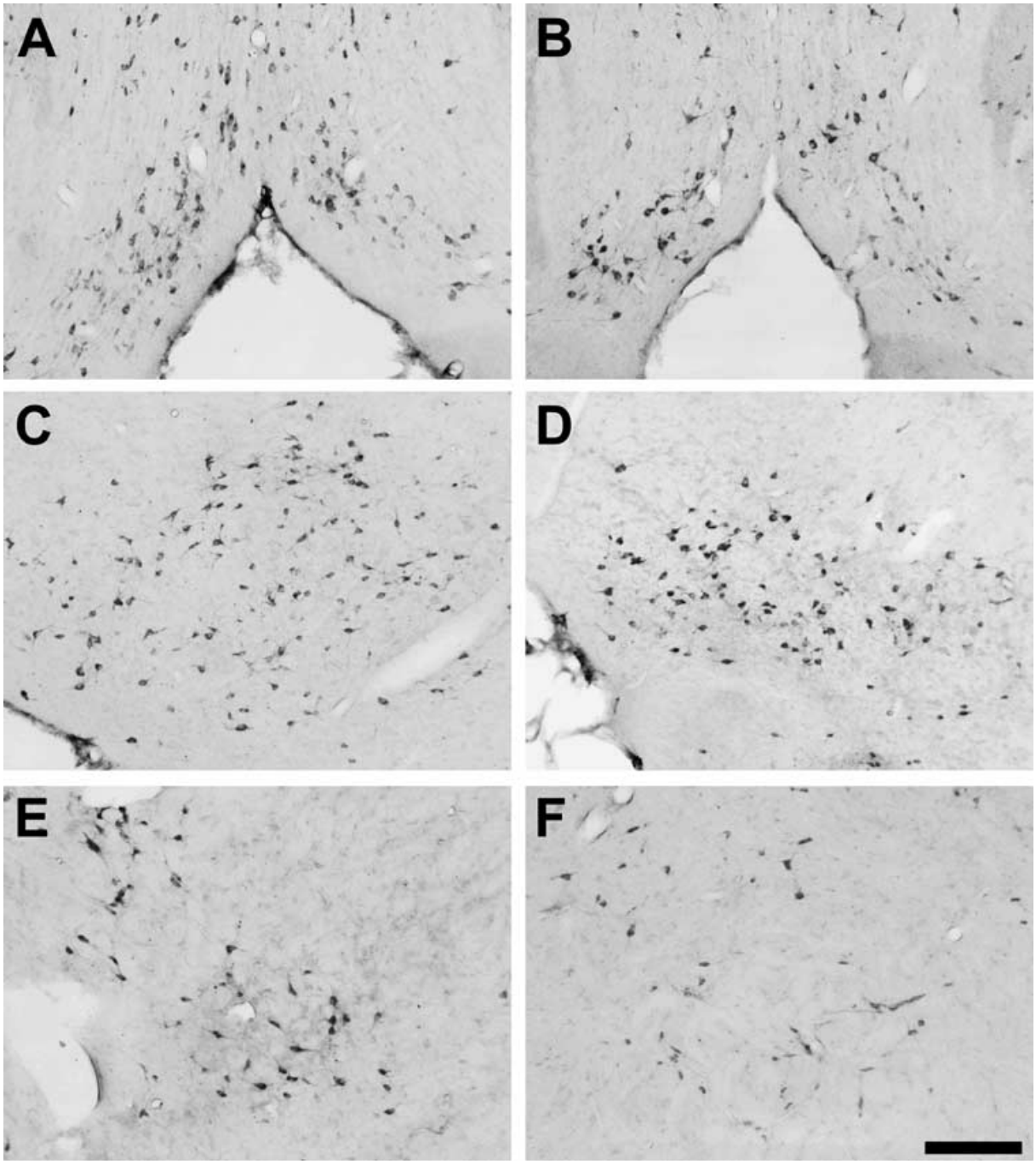

FIG. 6. Choline acetyl-transferase immunostaining in the vertical (A and B) and horizontal (C and D) limbs of the diagonal band of Broca and the nucleus basalis magnocellularis (E and F) in rats given vehicle treatment (left panels) or intra-SCN injections of 192 IgG-saporin (right panels). Scale bar, 200 μm.

TABLE 2. Number of immunoreactive cells to ChAT in the basal forebrain

	Control intra-SCN ($n = 7$)	Saporin intra-SCN ($n = 7$)
vDBB	75 ± 5	$42 \pm 6^{*}$
hDBB	92 ± 14	68 ± 11
NBM	56 ± 3	$46 \pm 2^{*}$

$^{*}P < 0.05$ between 192 IgG-saporin treatment and control group for a given brain region (*t*-test).

cells in the SCN was not significantly different in control vs. lesioned animals (25 ± 5 vs. 20 ± 5 cells, $n = 7$ and 5, respectively; $t_{10} = 1.9$, $P > 0.05$; Fig. 7E and F).

Circadian studies

i.c.v. injections of 192 IgG-saporin

None of the animals exhibited overt motor or behavioural deficit. i.c.v. injection of 192 IgG-saporin did not markedly alter the pattern of wheel-running activity when rats were exposed to a light–dark cycle

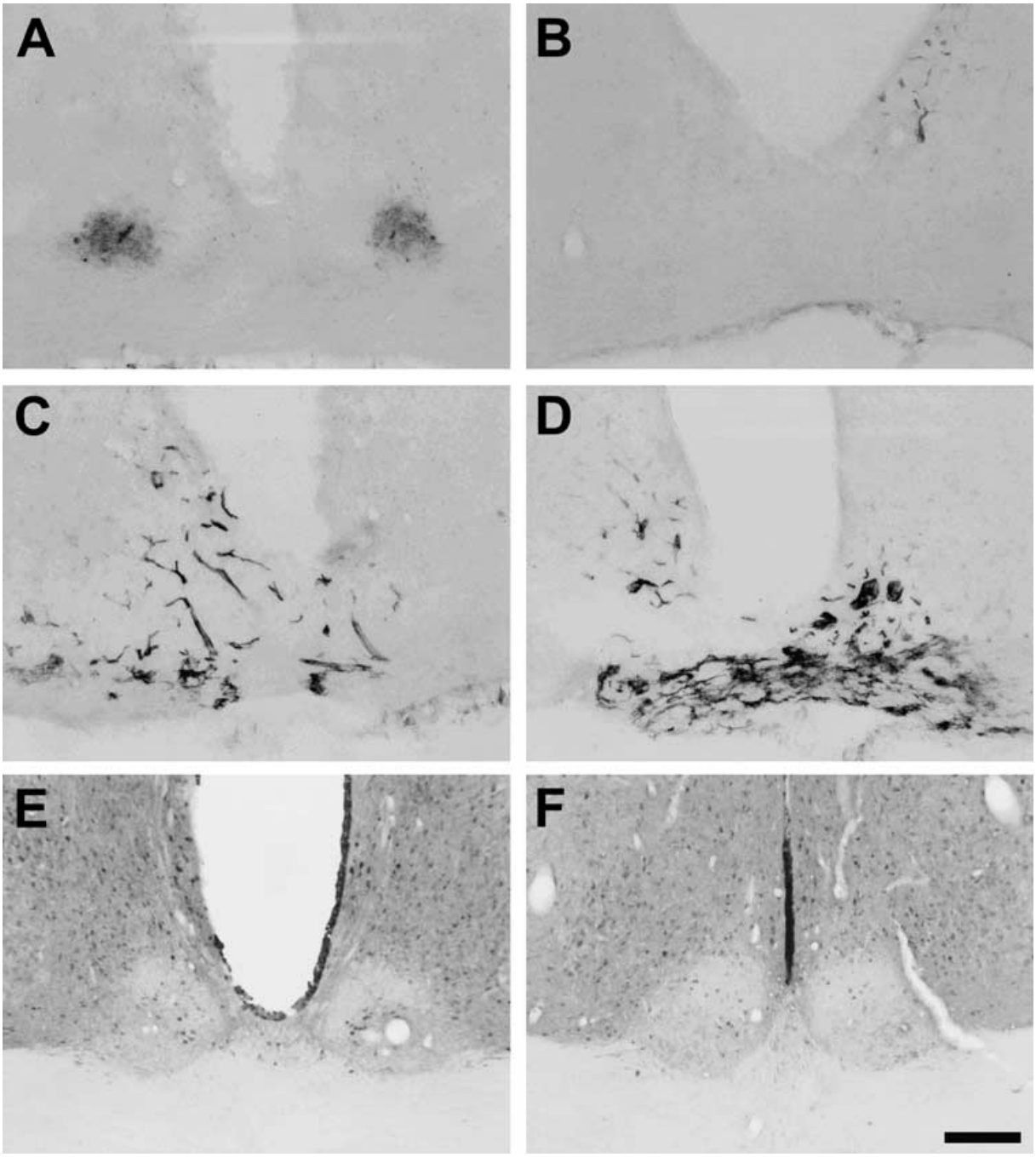

FIG. 7. p75 low-affinity nerve growth factor ($p75^{NGF}$) receptor (A–D) and calbindin-D28K (E and F) immunostaining in rats given vehicle treatment (A and E) or intra-SCN injections of 192 IgG-saporin (B, D and F). Panels B and C show representative lesioned animals with disappearance of $p75^{NGF}$ receptor immunostaining in the SCN or development of vascular $p75^{NGF}$ receptor immunostaining, respectively. Panel D shows the SCN region of one of the two animals that were excluded from the study because of extensive damage to the SCN and subsequent arrhythmicity. Scale bar, 200 μm.

(Fig. 8). Indeed, the times of activity onset and offset were similar before and after surgery ($F_{1,15} = 0.2$, $P > 0.1$ and $F_{1,15} = 0.5$, $P > 0.1$, respectively). A delay in the daily onsets of nocturnal activity was noted for both groups after surgery ($F_{1,15} = 36.85$, $P < 0.01$; see Table 3 for values). Moreover, i.c.v. injections of 192 IgG-saporin did not modify the number of wheel revolutions performed per day ($F_{1,15} = 0.8$, $P > 0.1$), during daytime ($F_{1,15} = 0.8$, $P > 0.1$) and nighttime ($F_{1,15} = 1.3$, $P > 0.1$; Table 3). The apparent increase in the level of nocturnal wheel-running activity before vs. after the i.c.v. surgery is probably related to the short duration the animals spent in their cages before surgery (see Methods). The endogenous period of free-running rhythm of locomotor activity was not altered by i.c.v. lesions in rats housed in constant darkness ($F_{1,38} = 0.2$, $P > 0.1$; Figs 8 and 9). Over the three intervals of measurement, there was a lengthening of the endogenous period (from 24.2 to 24.4 h) in the two groups of animals after exposure to the second light pulse (i.e. at CT14; $F_{2,38} = 3.9$, $P < 0.05$). Clear differences were observed for light-induced phase shifts of locomotor activity rhythm (Figs 9A, B, E and F, and 10). A light pulse administered at CT21 induced lower phase advances after i.c.v. injections of 192 IgG-saporin in comparison with the control

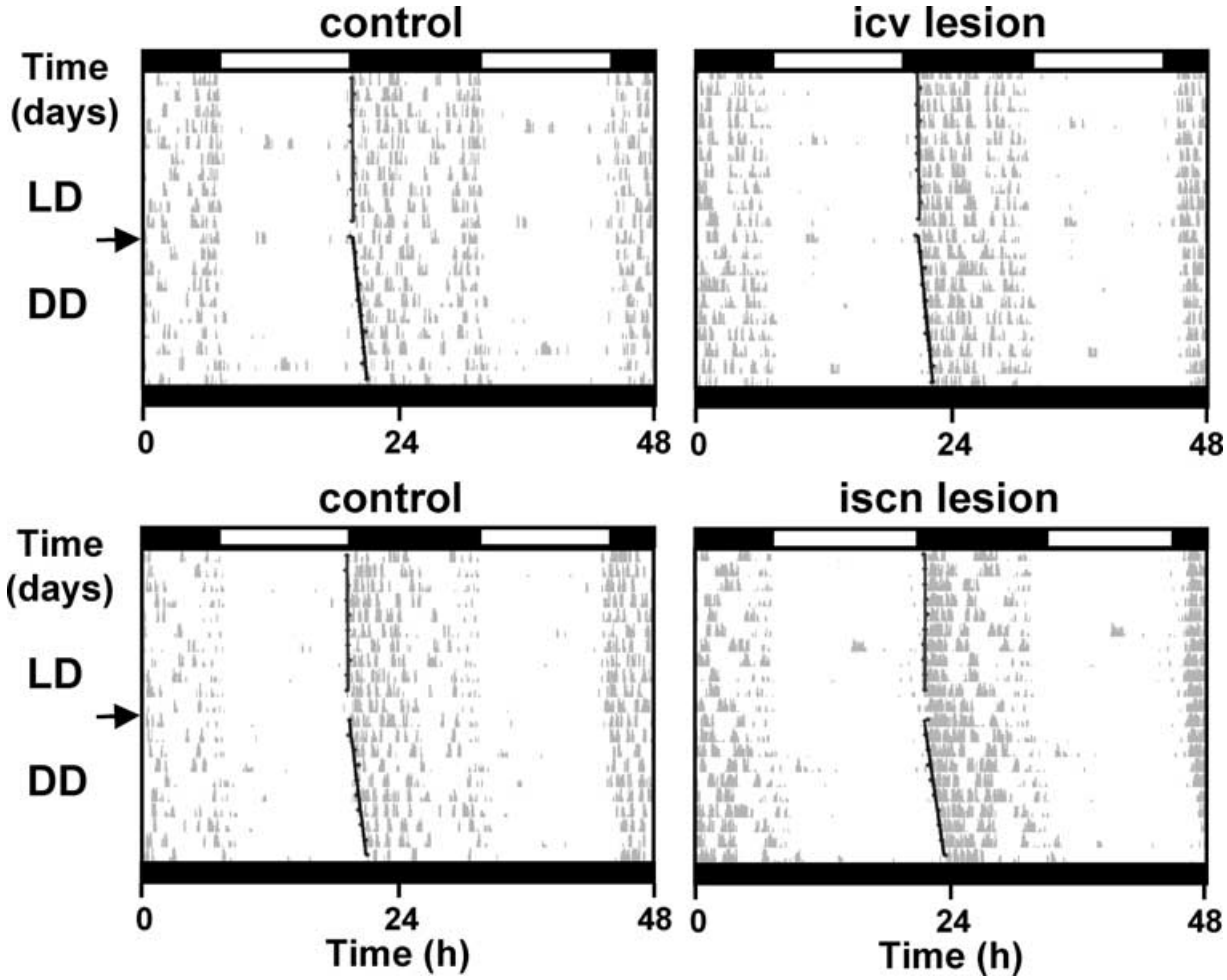

FIG. 8. Wheel-running activity in four rats given vehicle treatment (left panels), i.c.v. injections of 192 IgG-saporin (upper right panel) or intra-SCN injections (iscn) of 192 IgG-saporin (lower right panel). The rats were exposed successively to 10 days of 12 : 12-h light–dark cycle (LD) and 10 days of constant darkness (DD). Successive 24-h periods are double-plotted (48-h horizontal time scale). Arrows indicate the change in lighting conditions. For a given lighting condition, daily light and dark periods are indicated by horizontal light-shaded and dark-shaded bars above the corresponding period.

TABLE 3. Timing of locomotor activity and wheel revolutions performed per day

Parameter	Control i.c.v. ($n = 9$)	Saporin i.c.v. ($n = 12$)	Control intra-SCN ($n = 7$)	Saporin intra-SCN ($n = 7$)
Daily onset time				
Before lesion	19:40 h ± 20 min	19:40 h ± 10 min	19:00 h ± 05 min	19:00 h ± 05 min
After lesion	20:10 h ± 10 min	20:30 h ± 10 min	19:00 h ± 05 min	19:00 h ± 10 min
Daily offset time				
Before lesion	07:10 h ± 10 min	07:10 h ± 05 min	07:20 h ± 05 min	07:10 h ± 05 min
After lesion	07:10 h ± 05 min	07:10 h ± 05 min	07:50 h ± 20 min	07:30 h ± 10 min
Daily activity (wheel revolutions per day)				
Before lesion	517 ± 74	499 ± 68	1645 ± 207	1419 ± 215
After lesion	906 ± 181	1132 ± 124	1357 ± 221	979 ± 337
Diurnal activity (wheel revolutions per day)				
Before lesion	88 ± 27	73 ± 21	134 ± 26	108 ± 21
After lesion	69 ± 17	46 ± 8	66 ± 20	45 ± 12
Nocturnal activity (wheel revolutions per day)				
Before lesion	429 ± 52	426 ± 49	1511 ± 185	1311 ± 210
After lesion	837 ± 166	1086 ± 122	1291 ± 228	934 ± 327

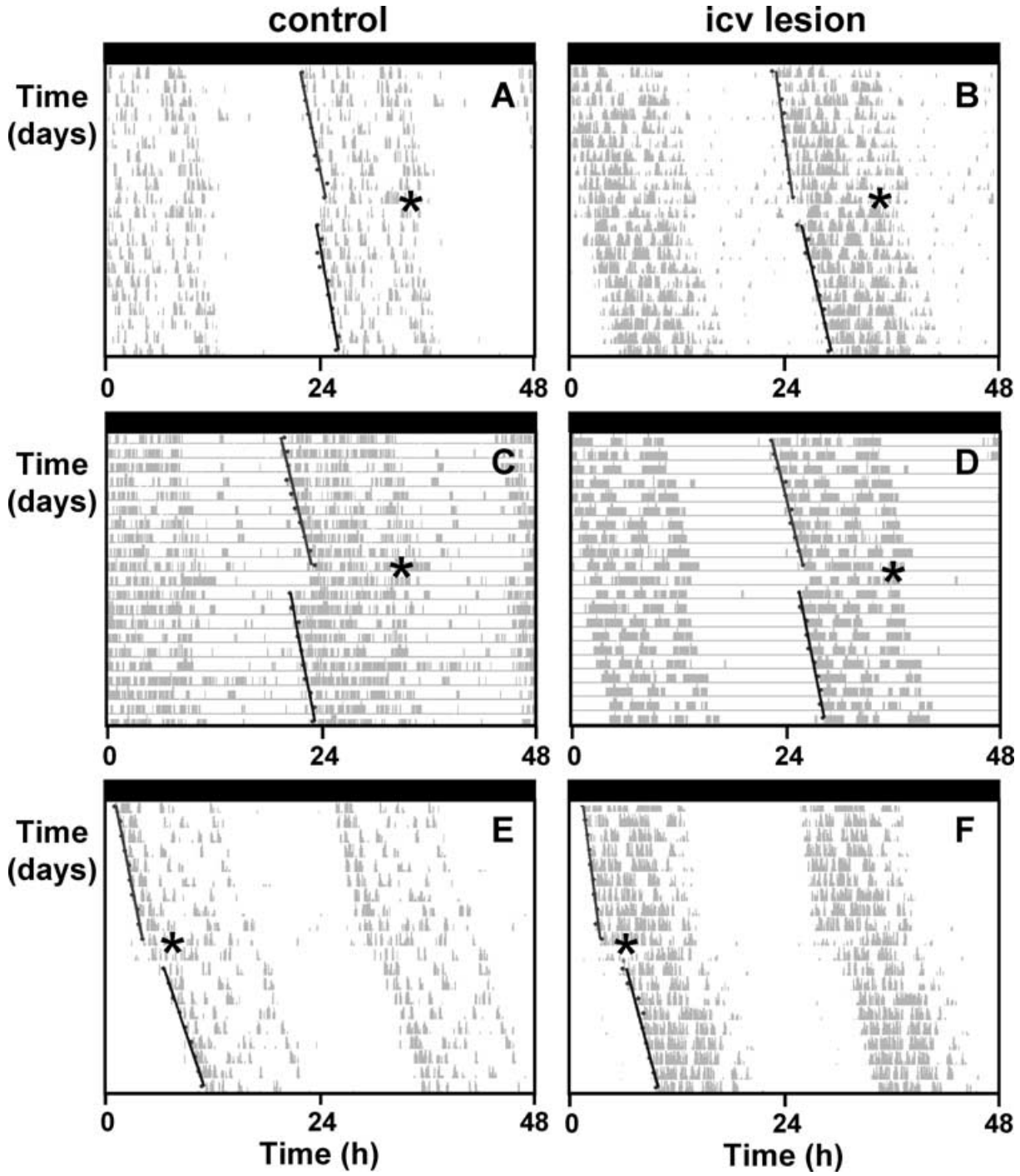

FIG. 9. Wheel-running activity (A, B, E and F) and body temperature (C and D) in six rats housed in constant darkness and given vehicle (left panels) or i.c.v. 192 IgG-saporin (right panels) injections. In panels A–D, the rats were exposed to light pulse (100 lux for 30 min) at circadian time (CT) 21, leading to subsequent phase advances. Note the lower magnitude of the phase advances in i.c.v. lesioned rats (B and D) compared with those in the controls (A and C). In panels E and F, the rats were exposed to light pulse (100 lux for 30 min) at CT14, leading to subsequent phase delays. Note the larger magnitude of the phase delays in the i.c.v. lesioned rat (F) compared with that of the control animal (E). Successive 24-h periods are double-plotted (48-h horizontal time scale). Stars indicate the time of light exposure.

group (60 ± 6 vs. 102 ± 10 min, $n = 12$ and 9, respectively; $t_{19} = 3.6$, $P < 0.001$; Figs 9A and B, and 10). Similar results for light-induced phase advances were obtained with data of core temperature (65 ± 6 vs. 99 ± 8 min, $n = 9$ and 7, respectively; $t_{14} = 3.0$, $P = 0.01$; Fig. 9C and D; the lower numbers of animals for temperature are due to transmitter failure). By contrast, a light pulse applied at CT14 resulted in phase delays of the circadian rhythms in the lesioned animals larger than in controls (-126 ± 12 vs. -96 ± 8 min, $n = 12$ and 9, respectively; $t_{19} = 2.1$, $P < 0.05$; Figs 9E and F, and 10). Only a trend for a difference was noted for light-induced phase delays of body temperature rhythm (-117 ± 7 vs. -98 ± 7 min, $n = 9$ and 7, respectively; $t_{19} = 1.6$, $P > 0.1$).

Intra-SCN injections of 192 IgG-saporin

Intra-SCN injections of 192 IgG-saporin did not alter the wheel-running pattern in rats exposed to a light–dark cycle (Fig. 8). Neither

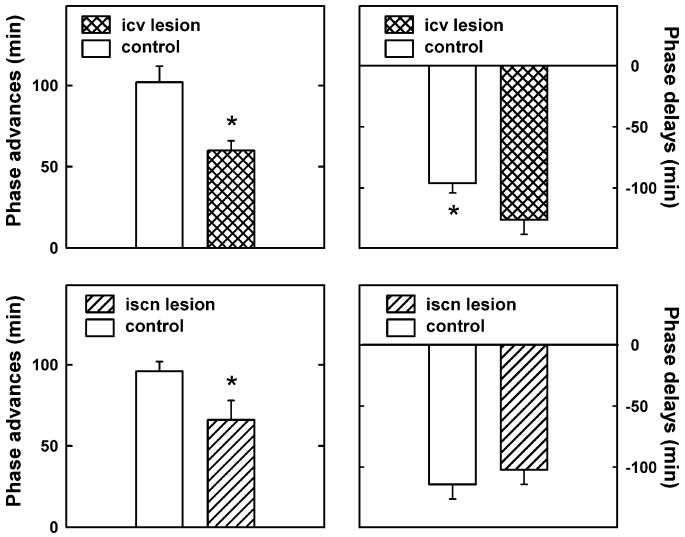

FIG. 10. Light-induced phase shifts in circadian activity rhythms of rats injected with vehicle (control), i.c.v. 192 IgG-saporin (i.c.v. lesion) or intra-SCN 192 IgG-saporin (iscn lesion). Positive and negative values are advances and delays, respectively. Values are means ± SEM. $^{*}P < 0.05$ compared with the other treatment.

the time of activity onsets nor that of the offsets were altered by the treatment ($F_{1,12} = 0.1$, $P > 0.1$ and $F_{1,12} = 1.5$, $P > 0.1$, respectively). We detected only a significant delay in the activity offset for both groups after surgery ($F_{1,12} = 8.5$, $P = 0.01$; see Table 3 for values). Intra-SCN lesions of 192 IgG-saporin did not significantly affect the number of wheel revolutions performed per day ($F_{1,12} = 0.9$, $P > 0.1$), during daytime ($F_{1,12} = 1.0$, $P > 0.1$) and nighttime ($F_{1,12} = 0.8$, $P > 0.1$; Table 3). Independently of the interval considered in constant darkness, there was a slight but significant reduction of the endogenous period in rats treated with intra-SCN 192 IgG-saporin compared with control animals (24.16 ± 0.01 vs. 24.30 ± 00.01 h, $n = 7$ in both groups; $F_{1,24} = 5.3$, $P < 0.05$). In response to light exposure at CT21, there were lower phase advances of locomotor activity rhythm in rats injected with 192 IgG-saporin in the SCN region compared with controls (66 ± 12 vs. 96 ± 6 min, respectively, $n = 7$ in both groups; $t_{12} = 2.4$, $P < 0.05$; Figs 10 and 11). A similar decrease was observed with data for core temperature (60 ± 13 vs. 101 ± 11 min, respectively, $n = 7$ in both groups; $t_{12} = 2.3$, $P < 0.05$). A light pulse applied at CT14 led to similar phase delays of locomotor activity rhythm in lesioned vs. control animals (−102 ± 12 vs. −114 ± 12 min, respectively, $n = 7$ in both groups; $t_{12} = 0.7$, $P > 0.1$; Fig. 10) and to similar delays of core temperature rhythm in the two groups of rats (−97 ± 10 vs. −104 ± 13 min, respectively, $n = 7$ in both groups; $t_{12} = 0.4$, $P > 0.1$).

Discussion

Our study suggests that lesions of the cholinergic, $p75^{NGF}$ receptor-expressing fibres that project from the basal forebrain to the SCN alter responses of the biological clock to phase shifting effects of light.

Assessment of cholinergic lesions

192 IgG-saporin injected i.c.v. leads to the destruction of cholinergic neurons in the basal forebrain, as assessed by the complete loss of AChE staining in the frontoparietal cortex. Indeed, AChE is predominantly found in cholinergic cells (Butcher & Woolf, 1984), even if AChE is not a selective marker for cholinergic neurons (Satoh *et al*., 1983). Nevertheless, this method has been commonly used to establish a loss of cholinergic fibres and terminals in the cerebral cortices, and to confirm the efficacy of lesions induced by i.c.v. injections of 192 IgG-saporin (Holley *et al*., 1994; Lehmann *et al*., 2000). The extensive loss of cholinergic fibres in the cortices and hippocampus indicates that most cholinergic neurons of the basal forebrain and projecting to the cortices and hippocampus are damaged after i.c.v. injection of 192 IgG-saporin. This specific cholinergic depletion leads to deficits in several cognitive tasks, including learning and memory tasks (Leanza *et al*., 1995; Lehmann *et al*., 2000).

Because of a weak AChE staining in the SCN, we were unable to confirm a loss of cholinergic neurons projecting to the SCN by densitometric analysis of AChE-positive products. Given that the SCN exhibits a very intense immunolabelling for $p75^{NGF}$ receptor in its ventrolateral region (Bina *et al*., 1997; Moga, 1998; Beaulé &

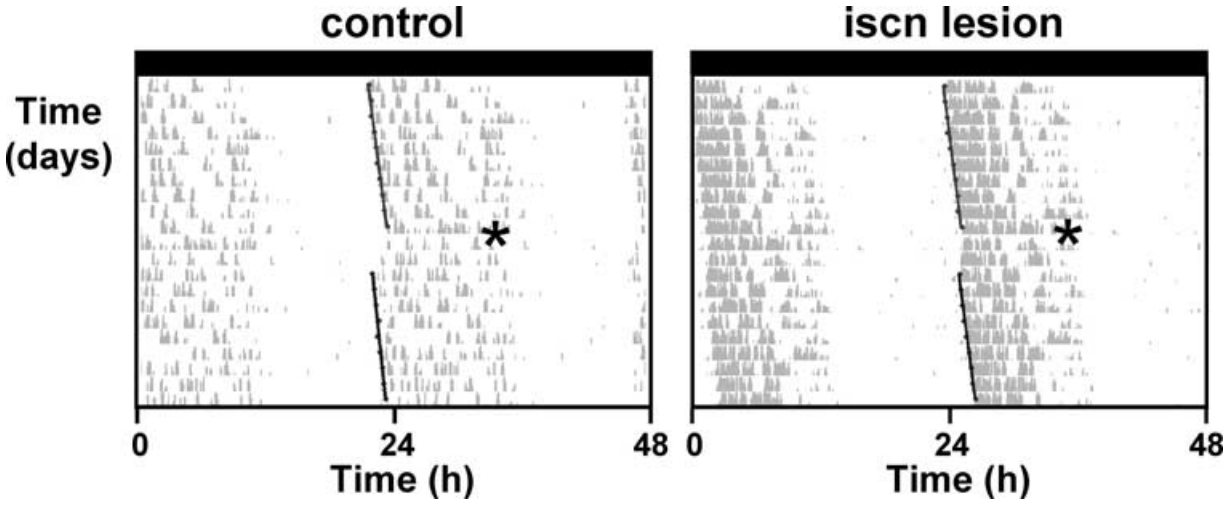

FIG. 11. Wheel-running activity in two rats housed in constant darkness and given vehicle (control) or intra-SCN 192 IgG-saporin (iscn lesion) injections. The rats were exposed to light pulse (100 lux for 30 min) at circadian time (CT) 21, leading to subsequent phase advances. Note the lower magnitude of the phase advance in the iscn lesioned rat (right panel) compared with that in the control animal (left panel). Successive 24-h periods are double-plotted (48-h horizontal time scale). Stars indicate the time of light exposure.

Amir, 2001), we performed $p75^{NGF}$ receptor immunocytochemistry to assess the extent of the cholinergic lesion within the SCN. In the central nervous system, $p75^{NGF}$ receptors can be found on both cell bodies and neuron terminals (Yan & Johnson, 1989; Hartig *et al*., 1998). Kiss and colleagues suggested a colocalization of $p75^{NGF}$ receptors with VIP in the SCN neurons (Kiss *et al*., 1993). However, 192 IgG-saporin, injected either i.c.v. or in the SCN region at doses that abolish $p75^{NGF}$ receptor immunoreactivity, does not alter VIP immunoreactivity in the SCN (Moga, 1998; the present study). Moreover, in contrast to a previous study (Beaulé & Amir, 2002), no significant decrease of cells expressing CalB was detected in the SCN after intrahypothalamic injections of 192 IgG-saporin. In addition, $p75^{NGF}$ receptor mRNA has never been identified within the SCN (Koh *et al*., 1989). Neuroanatomical studies also have clearly shown that $p75^{NGF}$ receptors in the SCN are located on axons terminals of basal cholinergic neurons and retinal ganglion cells (Bina *et al*., 1997). The neurotransmitter content of the ganglion cells expressing $p75^{NGF}$ receptor and projecting to the SCN is still unknown, albeit most probably not cholinergic (Bina *et al*., 1993, 1997). Together, these results indicate that the $p75^{NGF}$ receptors in the SCN area are more likely localized on afferent fibres rather than on VIP or other SCN neurons.

After i.c.v. 192 IgG-saporin injection, in spite of extensive damage ($\geq 90\%$) of $p75^{NGF}$ receptor immunoreactive (i.e. most likely cholinergic) neurons, half the $p75^{NGF}$ receptor immunostaining was still present in the SCN. The residual immunostaining in the SCN may be due to spared $p75^{NGF}$ receptor immunopositive terminals from retinal ganglion cells that would be less accessible. After intra-SCN injection of 192 IgG-saporin, a total loss of $p75^{NGF}$ receptor immunostaining was observed in the SCN. This demonstrates that, when injected locally, the toxin destroyed all $p75^{NGF}$ receptor immunopositive fibres and terminals in the SCN. Considering a potential indirect damage of a set of ganglion cells, it is possible that alterations of light-induced phase shifts are due to a loss of these noncholinergic retinohypothalamic fibres. It is, however, unlikely that this group of fibres plays a critical role in photic phase shifting. Specific destruction of these retinal projections has been associated with disruptive effects of constant light on circadian rhythms (Beaulé & Amir, 2001, 2002). Following intra-SCN injection of 192 IgG-saporin, the number of neurons immunoreactive to $p75^{NGF}$ receptor and ChAT was decreased to a variable extent in several regions of the basal forebrain (i.e. vDBB, hDBB and NBM). After this treatment, a direct lesion of cholinergic neurons close to the SCN is unlikely to be extensive because the highest reduction (40%) in the number of neurons immunoreactive to $p75^{NGF}$ receptor or ChAT was found in the furthest area (i.e. vDBB) from the injection site (see Table 1). Given that the cholinergic and $p75^{NGF}$ receptor immunoreactive afferents to the SCN come from vDBB, hDBB and NBM (Bina *et al*., 1993, 1997), the observed reduction in the number of forebrain cholinergic neurons after intra-SCN injection of 192 IgG-saporin probably reflects lesion through degeneration of terminals. According to our hypothesis (see above), the residual immunostaining of $p75^{NGF}$ receptor in the SCN after i.c.v. treatment is located on retinal afferents. Because the effects of 192 IgG-saporin on photic resetting were not more severe after intra-SCN injection compared with the i.c.v. route, this leads us to suggest that the effects of i.c.v. injection reflect more an impairment of $p75^{NGF}$ receptor-expressing (cholinergic) afferents to the SCN than the intra-SCN treatment in which both forebrain cholinergic terminals and retinal afferents expressing $p75^{NGF}$ receptors were fully lesioned. If correct, this interpretation suggests that retinal afferents may not be involved in the observed effects on light-induced phase shifts.

Modulation of phase shifting responses to light by neurons expressing $p75^{NGF}$ receptor

In our study, the lesioned rats were rhythmic under a 24-h light–dark cycle after i.c.v. or intra-SCN injection of saporin, thereby confirming previous data (Beaulé & Amir, 2002) and indicating that forebrain cholinergic projections and retinal afferents expressing $p75^{NGF}$ receptor are not critical for photic synchronization. In addition, we observed that destruction of the forebrain cholinergic projections after i.c.v. and intra-SCN injections of 192 IgG-saporin led to an important reduction of light-induced phase advances in the circadian rhythms of locomotor activity and core temperature. In accordance with this observation, mice with a targeted deletion of $p75^{NGF}$ receptor have been found to be less sensitive to the phase shifting effect of light (Golombek *et al*., 1996). Our data in rats provide support for the hypothesis that the anterior cholinergic projections modulate photic phase resetting of the SCN clock. In intact animals, a cholinergic stimulation would thus lead to an amplification of the light-induced phase advances, in accordance with many pharmacological data. When carbachol is administered i.c.v. in late subjective night in rats, mice or hamsters, or nicotine injected in late night in rats, they induce phase advances of behavioural rhythms (e.g. Mistlberger & Rusak, 1986; Wee *et al*., 1992).

During the early subjective night, we found an increase in light-induced phase delays after i.c.v. injection of 192 IgG-saporin. This therefore suggests either an inhibitory or a counteracting (phase advancing?) role of the anterior cholinergic projections on light-induced phase delays in intact animals. Intra-SCN injections of 192 IgG-saporin, however, had no significant effect on light-induced phase delays. Similarly, a reduction of light-induced c-FOS expression in the SCN has been noted after i.c.v. injections of 192 IgG-saporin, but not after intrahypothalamic injections (Beaulé & Amir, 2002). These discrepancies according to the route of immunotoxin administration may be related to the extensive destruction of the forebrain cholinergic fibres after i.c.v. injection or to the destruction of noncholinergic fibres expressing $p75^{NGF}$ receptors that would be spared after intra-SCN injection, but damaged after an i.c.v. injection. For instance, noncholinergic fibres expressing $p75^{NGF}$ receptors are found in the olivary pretectal nucleus and the intergeniculate leaflet (Beaulé & Amir, 2002), two structures that may modulate photic inputs to the SCN.

Nevertheless, our results concerning light-induced phase delays (after i.c.v. and intra-SCN injections of immunotoxin) do not support the hypothesis that cholinergic stimulation has photic-like effects on the SCN clock during the early subjective night (Wee *et al*., 1992; Colwell *et al*., 1993; O'Hara *et al*., 1998). Rather, our data support the view that cholinergic stimulation leads to phase advances during the whole night, as assessed *in vivo* in mice after direct administration of carbachol into the SCN region (Abbott *et al*., 2002) and *in vitro* in SCN slices of rats in response to various cholinergic agonists (Trachsel *et al*., 1995; Liu & Gillette, 1996). Thus, it seems that *in vitro*, the phase resetting effects of acetylcholine are translated into phase advances of the clock during the entire subjective night. Also, *in vivo* cholinergic stimulation in the late subjective night consistently leads to phase advances (Mistlberger & Rusak, 1986; Wee *et al*., 1992; Colwell *et al*., 1993; Abbott *et al*., 2002). By contrast, *in vivo* cholinergic activation in the early night may induce advances or delays according to various parameters, including the subtypes of cholinergic receptors, the route of administration and the species considered.

In comparison with *in vitro* slices of SCN that lack normal afferent inputs, the *in vivo* sensitivity of the SCN clock to cholinergic stimulation may depend on interaction with other neurotransmitter systems, especially with glutamatergic fibres transmitting photic information to the SCN. Such an interaction between acetylcholine and glutamate

may occur in intracellular and/or intercellular signalling pathways involving nitric oxide (Liu & Gillette, 1996). Indeed, it has been shown *in vitro* that nocturnal cholinergic stimulation of muscarinic receptors can reset the SCN clock by stimulating guanylyl cyclase, generating cGMP and activating cGMP-dependent protein kinase (Liu *et al*., 1997). This effect probably involves nitric oxide, which modulates clock resetting in response to nocturnal glutamatergic signals. Nitric oxide would act as a tonic intercellular signal that determines the basal level of cGMP and thus the state of cholinergic sensitivity (Artinian *et al*., 2001). The intense immunolabelling for $p75^{NGF}$ receptors in the SCN is restricted to its ventro-lateral region receiving retinal glutamatergic inputs. It is therefore likely that interactions between cholinergic and glutamatergic pathways occur within the SCN. Because the cholinergic basal forebrain also receives retinal projections (Youngstrom *et al*., 1991; Bina *et al*., 1993), such neurochemical interactions might also occur in the basal forebrain.

Conclusion and perspectives

The present study suggests an involvement of the forebrain cholinergic system in the phase resetting properties of light, whereas retinal afferents expressing $p75^{NGF}$ receptors probably have only a minor role. A high depletion of $p75^{NGF}$ receptor-expressing (i.e. most likely cholinergic) forebrain neurons resulted in a 40% decrease in light-induced phase advances, whereas light-induced phase delays were increased by 30%. A lesion with 192 IgG-saporin restricted to the SCN also led to a 30% decrease in light-induced phase advances, without significant effect on light-induced phase delays.

The cholinergic neurons in the basal forebrain and those originating from the pontine tegmentum are implicated in the regulation of sleep and arousal. In rats, depletion of forebrain acetylcholine after i.c.v. injection of 192 IgG-saporin has been shown to impair the daily distribution of sleep and vigilance states and to reduce EEG across all frequency bands (Kapas *et al*., 1996). Because our study suggests that the anterior cholinergic projections have a modulatory role on photic phase resetting, these cholinergic projections can be viewed as components of a feedback loop within the neural network underlying the regulation of sleep and wakefulness, and circadian timing (Bina *et al*., 1993; Kapas *et al*., 1996). The possible implication of the posterior cholinergic projections in the circadian timing system deserves further experimentation.

Acknowledgements

We wish to thank Dr H. Dardente for helpful comments on the manuscript. We are grateful to S. Gourmelen for help with the maintenance of experimental animals and actimetry set-up. We also thank Dr R. M. Buijs (Netherlands Institute for Brain Research, Amsterdam) for the gift of the VIP antiserum. The present study was funded in part by a fellowship from Sanofi-Synthélabo (C.E.) and a 'crédit exceptionnel pour jeunes équipes' from CNRS (E.C.).

Abbreviations

AChE, acetylcholinesterase; a.u., arbitrary units; i.c.v., intracerebroventricular; CalB, calbindin-D28K; ChAT, choline acetyl-transferase; CT, circadian time DD, constant darkness; hDBB, vertical limb of the diagonal band of Broca; LD, light–dark cycle; NBM, nucleus basalis magnocellularis; OD, optical density; SCN, suprachiasmatic nucleus; vDBB, horizontal limb of the diagonal band of Broca; VIP, vasoactive intestinal peptide; ZT, Zeitgeber time.

References

Abbott, S.M., Buchanan, G.F., Chang, Q., Gold, P.E. & Gillette, M.U. (2002) Deciphering the role of the cholinergic input to the mammalian circadian clock. *Soc. Res. Biol. Rhythms Abs.*, **8**, 76.

Artinian, L.R., Ding, J.M. & Gillette, M.U. (2001) Carbon monoxide and nitric oxide: interacting messengers in muscarinic signaling to the brain's circadian clock. *Exp. Neurol.*, **171**, 293–300.

Beaulé, C. & Amir, S. (2001) Photic regulation of circadian rhythms and the expression of p75 neurotrophin receptor immunoreactivity in the suprachiasmatic nucleus in rats. *Brain Res.*, **894**, 301–306.

Beaulé, C. & Amir, S. (2002) Effect of 192 IgG-saporin on circadian activity rhythms, expression of P75 neurotrophin receptors, calbindin-D28K, and light-induced Fos in the suprachiasmatic nucleus in rats. *Exp. Neurol.*, **176**, 377–389.

Bina, K.G., Rusak, B. & Semba, K. (1993) Localization of cholinergic neurons in the forebrain and brainstem that project to the suprachiasmatic nucleus of the hypothalamus in the rat. *J. Comp. Neurol.*, **335**, 295–307.

Bina, K.G., Rusak, B. & Semba, K. (1997) Sources of p75-nerve growth factor receptor-like immunoreactivity in the rat suprachiasmatic nucleus. *Neuroscience*, **77**, 461–472.

Butcher, L.L. & Woolf, N.J. (1984) Histochemical distribution of acetylcholinesterase in the central nervous system: clues to the localization of cholinergic neurons. In Björklund, A., Hökfelt, T. & Kuhar, M.J. (eds), *Handbook of Chemical Neuroanatomy*, Vol. 3: *Classical Transmitters and Receptors in the CNS.* Elsevier Science, Amsterdam, pp. 1–50.

Cantarella, G., Lempereur, L., Presta, M., Ribatti, D., Lombardo, G., Lazarovici, P., Zappala, G., Pafumi, C. & Bernardini, R. (2002) Nerve growth factor–endothelial cell interaction leads to angiogenesis in vitro and in vivo. *FASEB J.*, **16**, 1307–1309.

Colwell, C.S., Kaufman, C.M. & Menaker, M. (1993) Phase-shifting mechanisms in the mammalian circadian system: new light on the carbachol paradox. *J. Neurosci.*, **13**, 1454–1459.

Di Patre, P.L., Mathes, C.W. & Butcher, L.L. (1993) Differential visualization of cholinesterasic neuronal somata and fibers by use of modifications of acetylcholinesterase pharmacohistochemistry. *J. Histochem. Cytochem.*, **41**, 129–135.

Ferguson, S.A., Kennaway, D.J. & Moyer, R.W. (1999) Nicotine phase shifts the 6-sulphatoxymelatonin rhythm and induces c-Fos in the SCN of rats. *Brain Res. Bull.*, **48**, 527–538.

Golombek, D.A., Hurd, M.W., Lee, K.F. & Ralph, M.R. (1996) Mice lacking the $p75^{NGFR}$ receptor exhibit abnormal responses to light. *Biol. Rhythm Res.*, **27**, 409–418.

Hartig, W., Seeger, J., Naumann, T., Brauer, K. & Bruckner, G. (1998) Selective in vivo fluorescence labelling of cholinergic neurons containing p75 (NTR) in the rat basal forebrain. *Brain Res.*, **808**, 155–165.

Holley, L.A., Wiley, R.G., Lappi, D.A. & Sarter, M. (1994) Cortical cholinergic deafferentation following the intracortical infusion of 192 IgG-saporin: a quantitative histochemical study. *Brain Res.*, **663**, 277–286.

Kapas, L., Obal, F. Jr, Book, A.A., Schweitzer, J.B., Wiley, R.G. & Krueger, J.M. (1996) The effects of immunolesions of nerve growth factor-receptive neurons by 192 IgG-saporin on sleep. *Brain Res.*, **712**, 53–59.

Kawano, H., Decker, K. & Reuss, S. (1996) Is there a direct retina-raphe-suprachiasmatic nucleus pathway in the rat? *Neurosci. Lett.*, **212**, 143–146.

Keefe, D.L., Earnest, D.J., Nelson, D., Takahashi, J.S. & Turek, F.W. (1987) A cholinergic antagonist, mecamylamine, blocks the phase-shifting effects of light on the circadian rhythm of locomotor activity in the golden hamster. *Brain Res.*, **403**, 308–312.

Kiss, J. & Halasz, B. (1996) Synaptic contacts between cholinergic afferents and suprachiasmatic neurones of the rat. *Neuroreport*, **7**, 1961–1964.

Kiss, J., Patel, A.J. & Halasz, B. (1993) Colocalization of NGF receptor with VIP in rat suprachiasmatic neurones. *Neuroreport*, **4**, 1315–1318.

Koh, S., Oyler, G.A. & Higgins, G.A. (1989) Localization of nerve growth factor receptor messenger RNA and protein in the adult rat brain. *Exp. Neurol.*, **106**, 209–221.

Leanza, G., Nilsson, O.G., Wiley, R.G. & Bjorklund, A. (1995) Selective lesioning of the basal forebrain cholinergic system by intraventricular 192 IgG-saporin: behavioural, biochemical and stereological studies in the rat. *Eur. J. Neurosci.*, **7**, 329–343.

Lehmann, O., Jeltsch, H., Lehnardt, O., Pain, L., Lazarus, C. & Cassel, J.C. (2000) Combined lesions of cholinergic and serotonergic neurons in the rat brain using 192 IgG-saporin and 5, 7-dihydroxytryptamine: neurochemical and behavioural characterization. *Eur. J. Neurosci.*, **12**, 67–79.

Levey, A.I., Wainer, B.H., Rye, D.B., Mufson, E.J. & Mesulam, M.M. (1984) Choline acetyltransferase-immunoreactive neurons intrinsic to rodent cortex and distinction from acetylcholinesterase-positive neurons. *Neuroscience*, **13**, 341–353.

Liu, C., Ding, J.M., Faiman, L.E. & Gillette, M.U. (1997) Coupling of muscarinic cholinergic receptors and cGMP in nocturnal regulation of the suprachiasmatic circadian clock. *J. Neurosci.*, **17**, 659–666.

Liu, C. & Gillette, M.U. (1996) Cholinergic regulation of the suprachiasmatic nucleus circadian rhythm via a muscarinic mechanism at night. *J. Neurosci.*, **16**, 744–751.

Meijer, J.H., van der Zee, E. & Dietz, M. (1988) The effects of intraventricular carbachol injections on the free- running activity rhythm of the hamster. *J. Biol. Rhythms*, **3**, 333–348.

Miller, M.M. & Billiar, R.B. (1986) Relationship of putative nicotinic cholinergic receptors in the suprachiasmatic nucleus to levels of pineal serotonin N-acetyltransferase activity in the normally cycling female, the male, and the ovariectomized rat. *J. Pineal Res.*, **3**, 159–168.

Mistlberger, R.E. & Rusak, B. (1986) Carbachol phase shifts circadian activity rhythms in ovariectomized rats. *Neurosci. Lett.*, **72**, 357–362.

Moga, M.M. (1998) 192 IgG-saporin abolishes p75 neurotrophin receptor immunoreactivity in rat SCN. *Neuroreport*, **9**, 3197–3200.

Morin, L.P. (1994) The circadian visual system. *Brain Res. Rev.*, **67**, 102–127.

Murakami, N., Takahashi, K. & Kawashima, K. (1984) Effect of light on the acetylcholine concentrations of the suprachiasmatic nucleus in the rat. *Brain Res.*, **311**, 358–360.

O'Hara, B.F., Edgar, D.M., Cao, V.H., Wiler, S.W., Heller, H.C., Kilduff, T.S. & Miller, J.D. (1998) Nicotine and nicotinic receptors in the circadian system. *Psychoneuroendocrinology*, **23**, 161–173.

Paxinos, G. & Watson, C. (1986) *The Rat Brain in Stereotaxic Coordinates*. Academic Press, New York.

Pitrosky, B., Kirsch, R., Malan, A., Mocaer, E. & Pévet, P. (1999) Organization of rat circadian rhythms during daily infusion of melatonin or S20098, a melatonin agonist. *Am. J. Physiol.*, **277**, R812–R828.

van den Pol, A.N. & Tsujimoto, K.L. (1985) Neurotransmitters of the hypothalamic suprachiasmatic nucleus: immunocytochemical analysis of 25 neuronal antigens. *Neuroscience*, **15**, 1049–1086.

Satoh, K., Armstrong, D.M. & Fibiger, H.C. (1983) A comparison of the distribution of central cholinergic neurons as demonstrated by acetylcholinesterase pharmacohistochemistry and choline acetyltransferase immunohistochemistry. *Brain Res. Bull.*, **11**, 693–720.

Shen, H. & Semba, K. (1994) A direct retinal projection to the dorsal raphe nucleus in the rat. *Brain Res.*, **635**, 159–168.

Takeuchi, Y., Katoh, Y. & Takahashi, K. (1993) Classical acetylcholine receptors do not play a direct role in neuronal transmission of photic information in the suprachiasmatic nucleus in rats. *Neurosci. Lett.*, **158**, 71–74.

Trachsel, L., Heller, H.C. & Miller, J.D. (1995) Nicotine phase-advances the circadian neuronal activity rhythm in rat suprachiasmatic nuclei explants. *Neuroscience*, **65**, 797–803.

Wee, B.E., Anderson, K.D., Kouchis, N.S. & Turek, F.W. (1992) Administration of carbachol into the lateral ventricle and suprachiasmatic nucleus (SCN) produces dose-dependent phase shifts in the circadian rhythm of locomotor activity. *Neurosci. Lett.*, **137**, 211–215.

Yan, Q. & Johnson, E.M. (1989) Immunohistochemical localization and biochemical characterization of nerve growth factor receptor in adult rat brain. *J. Comp. Neurol.*, **290**, 585–598.

Youngstrom, T.G., Weiss, M.L. & Nunez, A.A. (1991) Retinofugal projections to the hypothalamus, anterior thalamus and basal forebrain in hamsters. *Brain Res. Bull.*, **26**, 403–411.

Zatz, M. & Brownstein, M.J. (1979) Intraventricular carbachol mimics the effects of light on the circadian rhythm in the rat pineal gland. *Science*, **203**, 358–361.

Zatz, M. & Herkenham, M.A. (1981) Intracerebroventricular carbachol mimics the phase shifting effects of light on the circadian rhythm of wheel-running activity. *Brain Res.*, **212**, 234–238.

van der Zee, E.A., Streefland, C., Strosberg, A.D., Schroder, H. & Luiten, P.G. (1991) Colocalization of muscarinic and nicotinic receptors in cholinoceptive neurons of the suprachiasmatic region in young and aged rats. *Brain Res.*, **542**, 348–352.

Zhang, Y., Zee, P.C., Kirby, J.D., Takahashi, J.S. & Turek, F.W. (1993) A cholinergic antagonist, mecamylamine, blocks light-induced Fos immunoreactivity in specific regions of the hamster suprachiasmatic nucleus. *Brain Res.*, **615**, 107–112.